

A VARIABLE FIDELITY OPTIMIZATION FRAMEWORK USING SECOND-ORDER MULTI-POINT ADDITIVE SCALING FUNCTIONS APPLIED TO AIRFOIL DESIGN

Qian Ruizhan*, Zhu Ziqiang**, Duan Zhuoyi*, Wei Jianlong***

*** The First Aircraft Institute of AVIC-I, Xi'an, 710089, China**

**** Beijing University of Aeronautics and Astronautics, Beijing, 100083, China**

Keywords: *variable fidelity optimization, scaling function, airfoil, Navier-Stokes equations*

Abstract

One of the most great barriers in practical implementation of standard optimization methods in engineering design problems, especially in aerodynamic optimization designs, is a potential high computational cost. Variable fidelity optimization methods, which combine high and low fidelity physics analyses, can converge to the high fidelity solution at a fraction of the computational cost of standard optimization methods performed on the high fidelity analyses alone. The scaling functions matching the low and high fidelity models in values and gradients play key roles in the whole optimization frameworks. Existing scaling functions most commonly are first-order multiplicative or additive, which can be insufficient to some problems.

In this paper, we propose a new second-order additive scaling function and present a Sequential Quadratic Programming (SQP) based variable fidelity optimization framework, which is carried out successfully on airfoil optimization designs. The proposed scaling function is a sum of quasi-Newton approximation of the high fidelity model and a term concerned to the low fidelity model and its quasi-Newton approximation. This paper also introduces a new set of design variables for airfoil optimization. Navier-Stokes equations evaluated on fine grids with high degree of convergence accuracy represent the high fidelity flow model, while Navier-Stokes equations evaluated on coarse grids with low

degree of convergence accuracy represent the low fidelity flow model. One-point and two-point optimization designs performed on RAE2822 airfoil are discussed. Compared to standard SQP optimization the presented optimization framework yields 58.64% and 71.18% CPU time reduction for one-point and two-point airfoil design, respectively. The study indicates the proposed optimization procedure can be applied in industry.

1 Introduction

During recent years, computational fluid dynamics (CFD) has brought about optimization method in aerodynamic design. A CFD analysis code is coupled with an optimization algorithm in such a way as to create a design tool. Aerodynamic quantities such as lift, drag, pitching moment are computed by the CFD code for a certain configuration and are used in defining an objective function to be minimized/maximized by the optimizer through automatically and gradually modification of its shape. Finally, the aerodynamic characteristics of a baseline configuration are improved [1][2][3]. This is a standard optimization procedure in aerodynamic design.

One of the most significant barriers in practical applications of these kinds of standard optimization methods is an enormous computational cost. Employing a lower-order flow model can save computational time, but the physical response of the design will not be optimum, and may even be adverse [4].

To save computational time while assure design quality, variable fidelity optimization, which combine high and low fidelity physics analyses, is a promising choice. Alexandrov et al proposed a general approach to design optimization, the first-order approximation and model management optimization (AMMO) framework, that integrates engineering and physical modeling concepts with trust region approach [5]. AMMO was applied to airfoil design, wing design [5] and multi-element airfoil optimization [6], resulted in enormous savings in terms of high-fidelity analysis. M.S. Eldred et al demonstrated that first-order consistency between the high and low model can be insufficient to achieve desirable convergence rates in practice and presented second-order additive, multipliable and combined corrections [7]. Shawn E. Gano et al developed second-order additive scaling methods based multilevel variable fidelity optimization approach applied to morphing unmanned aerial vehicle design [8].

The work in this paper is based on the first-order AMMO presented by Alexandrov et al. We propose a new second-order additive scaling function using approximated second-order information. The proposed scaling function satisfies first-order consistency between the high and low fidelity models at two points, increasing global accuracy of the correction and convergence rate of the optimization. We describe a variable fidelity optimization framework, using this scaling function, based on SQP and trust region approach, verified by analytical test problem and transonic airfoil designs.

2 Second order scaling function based AMMO

Mathematically, a constrained optimization problem can be stated as:

$$\begin{aligned} & \text{Minimize } f(x) \\ & \text{Subject to } c_i(x) = 0, \quad i \in E \\ & \quad \quad \quad c_i(x) \geq 0, \quad i \in I \end{aligned} \quad (1)$$

where x is the n -dimensional vector of design variables, f is objective function, c_i are constraint functions, E and I are the index sets

of the equality and inequality constraints, respectively.

Let f_{hi}, f_{lo} be high-fidelity and low-fidelity models of f , respectively. Let $c_{hi,i}, c_{lo,i}$ be high-fidelity and low-fidelity models of c_i , respectively. Problem (1) can be solved by solving a sequence of k trust region optimization sub-problems of the form.

$$\begin{aligned} & \text{minimize } \hat{f}^k(x) + \mu_k(\theta_k - 1)^2 \\ & \text{subject to } \theta_k c_{hi,i}(x_k) + \nabla c_{hi,i}(x_k)^T(x - x_k) \\ & \quad + t_{c,i} [c_{lo,i}(x) - c_{lo,i}(x_k) - \nabla c_{lo,i}(x_k)^T(x - x_k)] \\ & \quad = 0, i \in E \\ & \quad \theta_k c_{hi,i}(x_k) + \nabla c_{hi,i}(x_k)^T(x - x_k) \\ & \quad + t_{c,i} [c_{lo,i}(x) - c_{lo,i}(x_k) - \nabla c_{lo,i}(x_k)^T(x - x_k)] \\ & \quad \geq 0, i \in I \\ & \quad \|x - x_k\|_2^2 \leq \Delta_k^2 \\ & \quad 0 < \theta \leq 1 \end{aligned} \quad (2)$$

where the approximation model of $f(x)$ at k iteration is denoted as $\hat{f}^k(x)$, x_k is the center point of the trust region, μ_k is the penalty parameter, Δ_k is the trust region size, and the initial value for Δ at $k=0$ is user-defined. $\nabla c_{hi,i}(x_k)$ and $\nabla c_{lo,i}(x_k)$ are gradients of $c_{hi,i}(x)$ and $c_{lo,i}(x)$ at x_k , respectively. Variable θ_k is introduced to avoid the infeasibility of the trust region sub-problem [9].

The constraint functions are approximated using first-order multi-point scaling method. Here the multiple points mean the current iteration point x_k and the last iteration point x_{k-1} . The parameters, $t_{c,i}$, are defined as

$$t_{c,i} = \begin{cases} 0, & |c_{hi,i}(x_{k-1}) - c_{hi,i}(x_k) - \nabla c_{hi,i}(x_k)^T(x_{k-1} - x_k)| < \varepsilon \\ 0, & |c_{lo,i}(x_{k-1}) - c_{lo,i}(x_k) - \nabla c_{lo,i}(x_k)^T(x_{k-1} - x_k)| < \varepsilon \\ \frac{c_{hi,i}(x_{k-1}) - c_{hi,i}(x_k) - \nabla c_{hi,i}(x_k)^T(x_{k-1} - x_k)}{c_{lo,i}(x_{k-1}) - c_{lo,i}(x_k) - \nabla c_{lo,i}(x_k)^T(x_{k-1} - x_k)}, & \text{otherwise} \end{cases} \quad (3)$$

where ε is user-defined small positive number.

The trust region sub-problem (2) can be solved using SQP method.

We propose the second-order multi-point scaling function for objective function

$$\begin{aligned} \hat{f}^k(x) = & f_{hi}(x_k) + \nabla f_{hi}(x_k)^T(x - x_k) \\ & + \frac{1}{2}(x - x_k)^T B_{hi}(x_k)(x - x_k) \\ & + t_f \left[f_{lo}(x) - f_{lo}(x_k) - \nabla f_{lo}(x_k)^T(x - x_k) \right. \\ & \left. - \frac{1}{2}(x - x_k)^T B_{lo}(x_k)(x - x_k) \right] \end{aligned} \quad (4)$$

$$t_f = \begin{cases} 0, & f_{hi}(x_{k-1}) - f_{hi}(x_k) - \nabla f_{hi}(x_k)^T(x_{k-1} - x_k) \leq 0 \\ 0, & f_{lo}(x_{k-1}) - f_{lo}(x_k) - \nabla f_{lo}(x_k)^T(x_{k-1} - x_k) \leq 0 \\ 0, & \left| f_{hi}(x_{k-1}) - f_{hi}(x_k) - \nabla f_{hi}(x_k)^T(x_{k-1} - x_k) \right. \\ & \left. - \frac{1}{2}(x_{k-1} - x_k)^T B_{hi}(x_k)(x_{k-1} - x_k) \right| \leq \varepsilon \\ 0, & \left| f_{lo}(x_{k-1}) - f_{lo}(x_k) - \nabla f_{lo}(x_k)^T(x_{k-1} - x_k) \right. \\ & \left. - \frac{1}{2}(x_{k-1} - x_k)^T B_{lo}(x_k)(x_{k-1} - x_k) \right| \leq \varepsilon \\ \left[f_{hi}(x_{k-1}) - f_{hi}(x_k) - \nabla f_{hi}(x_k)^T(x_{k-1} - x_k) \right. \\ \left. - \frac{1}{2}(x_{k-1} - x_k)^T B_{hi}(x_k)(x_{k-1} - x_k) \right] / \\ \left[f_{lo}(x_{k-1}) - f_{lo}(x_k) - \nabla f_{lo}(x_k)^T(x_{k-1} - x_k) \right. \\ \left. - \frac{1}{2}(x_{k-1} - x_k)^T B_{lo}(x_k)(x_{k-1} - x_k) \right], & \text{otherwise} \end{cases} \quad (5)$$

where $\nabla f_{hi}(x_k)$ and $\nabla f_{lo}(x_k)$ are gradients of $f_{hi}(x)$ and $f_{lo}(x)$ at x_k , $B_{hi}(x_k)$ and $B_{lo}(x_k)$ are quasi-Newton approximations to the Hessian $\nabla^2 f_{hi}(x_k)$, $\nabla^2 f_{lo}(x_k)$, respectively.

$$\begin{aligned} \text{Let } B_k &= B_{hi}(x_k) \quad \nabla f_k = \nabla f_{hi}(x_k) \\ B_{k-1} &= B_{hi}(x_{k-1}) \quad \nabla f_{k-1} = \nabla f_{hi}(x_{k-1}) \end{aligned} \quad (6)$$

The damped BFGS update of B_k is defined by the following

$$\begin{aligned} B_k &= B_{k-1} - \frac{B_{k-1} s_k s_k^T B_{k-1}^T}{s_k^T B_{k-1} s_k} + \frac{\bar{y}_k \bar{y}_k^T}{s_k^T \bar{y}_k} \\ \bar{y}_k &= \begin{cases} y_k, & s_k^T y_k \geq 0.2 s_k^T B_{k-1} s_k \\ \mathcal{G}_k y_k + (1 - \mathcal{G}_k) B_{k-1} s_k, & s_k^T y_k < 0.2 s_k^T B_{k-1} s_k \end{cases} \\ \mathcal{G}_k &= \frac{0.8 s_k^T B_{k-1} s_k}{s_k^T B_{k-1} s_k - s_k^T y_k} \\ y_k &= \nabla f_k - \nabla f_{k-1} \\ s_k &= x_k - x_{k-1} \end{aligned} \quad (7)$$

The identity matrix I is used for B_0 prior to the first update.

The updating of $B_{lo}(x_k)$ may be deduced by analogy.

If $t_f \neq 0$, the second-order multi-point scaling function $\hat{f}^k(x)$ satisfies

$$\begin{aligned} \hat{f}^k(x_k) &= f_{hi}(x_k) \quad \nabla \hat{f}^k(x_k) = \nabla f_{hi}(x_k) \\ \hat{f}^k(x_{k-1}) &= f_{hi}(x_{k-1}) \quad \nabla \hat{f}^k(x_{k-1}) = \nabla f_{hi}(x_{k-1}) \end{aligned} \quad (8)$$

That is to say, the proposed scaling function satisfies first-order consistency between the high-fidelity and the low-fidelity models at the two successional iteration points, x_k and x_{k-1} . This provides a much more substantial correction capability over the existing first-order or second-order scaling functions.

When t_f becomes zero under four conditions in (5), the scaling function degenerates to BFGS approximation of high-fidelity model. This mechanism is devised for two purposes: keep the algorithm stable when high or low fidelity model is not convex; reduce the low-fidelity model evaluations at the late stage of the optimization.

Let $\Phi(x, \mu_k)$ be merit function for the high-fidelity problem

$$\Phi(x, \mu_k) = f_{hi}(x) + \mu_k \left[\sum_{i \in E} |c_{hi,i}(x)| + \sum_{i \in I} \max[0, -c_{hi,i}(x)] \right] \quad (9)$$

AMMO models the merit function by

$$\hat{\Phi}(x, \mu_k) = \hat{f}^k(x) + \mu_k \left[\sum_{i \in E} |\hat{c}_i^k(x)| + \sum_{i \in I} \max[0, -\hat{c}_i^k(x)] \right] \quad (10)$$

where

$$\begin{aligned} \hat{c}_i^k(x) &= c_{hi,i}(x_k) + \nabla c_{hi,i}(x_k)^T(x - x_k) \\ &+ t_{c,i} \left[c_{lo,i}(x) - c_{lo,i}(x_k) - \nabla c_{lo,i}(x_k)^T(x - x_k) \right] \end{aligned} \quad (11)$$

The SQP based second-order AMMO method is outlined bellow:

Initialize x_0, μ_0, Δ_0

Do $k = 0, 1, \dots$, until convergence

Construct $\hat{f}^k(x)$ and $\hat{c}_i^k(x)$ with second and first order matching at x_k , respectively;

Solve approximately the SQP problem (2);

Compute merit function $\Phi(x, \mu_k), \hat{\Phi}(x, \mu_k)$;

Update x_k, μ_k and Δ_k based on the values of $\Phi(x, \mu_k), \hat{\Phi}(x, \mu_k)$

End do

Details of the updating strategy can be found in [5][7][8].

In this work, gradient information is calculated using a centric finite difference defined as

$$\frac{\partial t}{\partial x_i} \approx \frac{t(x_i + \delta) - t(x_i - \delta)}{2\delta} \quad (12)$$

where t is either the objective or constraint function and δ is a small perturbation value for the design variables.

The choice of initial trust region size, Δ_0 , has a notable effect on the convergence rate of the AMMO algorithm. We suggest the following procedure to select Δ_0 : the solution to the low-fidelity problem, $x_{lo, \min}$, can be cheaply obtained by using SQP method; Δ_0 can be determined by the following

$$\Delta_0 = \|x_{lo, \min} - x_0\|_2 \quad (13)$$

3 Analytic test problem

We employ the standard Rosenbroke function as the high fidelity function (HFF) and perform the following optimization:

$$\begin{aligned} \text{Minimize } & f_{hi}(x) = 100(x_2 - x_1^2)^2 + (1 - x_1)^2 \\ \text{Subject to } & -2 \leq x_1 \leq 2 \\ & -2 \leq x_2 \leq 2 \end{aligned} \quad (14)$$

This high-fidelity problem has a theoretic minimum $f^* = 0$ at $(x_1^*, x_2^*) = (1, 1)$. M.S.Eldred et al define two “low-fidelity” Rosenbroke functions to examine different corrections [7]. The two low fidelity functions (LFF) are just the high fidelity function with two kinds of noise factors. The low fidelity function with offsets is

$$f_{lo}(x) = 100(x_2 - x_1^2 + 0.2)^2 + (0.8 - x_1)^2 \quad (15)$$

with a low-fidelity minimum at (0.8, 0.44).

The low fidelity function with scaling is

$$f_{lo}(x) = 100(1.25x_2 - x_1^2)^2 + (1 - 1.25x_1)^2 \quad (16)$$

with a low-fidelity minimum at (0.8, 0.512).

We add another low-fidelity function with both offsets and scaling

$$f_{lo}(x) = 100(1.25x_2 - x_1^2 + 0.2)^2 + (0.8 - 1.25x_1)^2 \quad (17)$$

with a low-fidelity minimum at (0.64, 0.16768).

The optimizations start from the initial point (-1.2, 1.0). The initial trust region size Δ_0 is calculated by the initial point and the low fidelity minimum points. Table 1 shows the results of the second-order AMMO and SQP method. For the three low fidelity functions, the proposed approach works well, converging to the high fidelity solution with far fewer high fidelity function evaluations than standard SQP method. In the case of low fidelity function with offsets, the reduction of high fidelity function evaluations is as great as 72.51%.

Table 1 Second-order AMMO results for Rosenbrok’s function

	LFF with offsets	LFF with scaling	LFF with offsets & scaling	SQP
x_1^*	1.0002	1.0003	0.9998	1.0000
x_2^*	1.0004	1.0005	0.9995	1.0000
f^*	4.62E-8	6.59E-8	5.84E-8	3.91E-12
HFF Evals	58	87	67	211
LFF Evals	245	1215	352	0
Δ_0	2.08	2.06	2.02	

4.1 Design Variables

This paper proposes a new set of design variables for airfoil optimization.

The design procedure starts with a baseline airfoil. New airfoil is generated by adding smooth perturbations on upper and lower surfaces of the baseline airfoil. The new airfoil geometry is represented by the following equations

$$\bar{y}_u(\bar{x}) = \bar{y}_{ub}(\bar{x}) \left(1 + \sum_{i=1}^{n_u} \delta_i P_i(\bar{x}) \right) \quad (18)$$

$$\bar{y}_l(\bar{x}) = \bar{y}_{lb}(\bar{x}) \left(1 + \sum_{i=n_u+1}^{n_u+n_l} \delta_i P_i(\bar{x}) \right) \quad (19)$$

where \bar{x} and \bar{y} are the dimensionless coordinates of the baseline airfoil, u and l denote upper and lower surface of the airfoil,

respectively, b denote baseline airfoil, P_i are Chebyshev or Legendre polynomials at $[0,1]$, n_u and n_l are the number of Chebyshev or Legendre polynomials added to the upper and lower surface, respectively. The weighting coefficients, δ_i , are the design variables. $n = n_u + n_l$ is the number of variables.

Because the Chebyshev or Legendre polynomials are used in airfoil parameterization, the optimization algorithm become more effective and the baseline airfoil is modified regularly.

In this investigation, twelve Chebyshev polynomials are selected in airfoil parameterization for RAE 2822 optimization ($n_u = n_l = 6$).

4.2 Flow Model

The two-dimensional Navier-Stokes equations read

$$\iint_{\Omega} \frac{\partial \mathbf{W}}{\partial t} d\Omega + \int_{\partial\Omega} \mathbf{F} n_x ds + \int_{\partial\Omega} \mathbf{G} n_y ds = 0 \quad (20)$$

where

$$\mathbf{W} = \begin{bmatrix} \rho \\ \rho u \\ \rho v \\ \rho E \end{bmatrix} \quad \mathbf{F} = \begin{bmatrix} \rho u \\ \rho u^2 + p + \sigma_x \\ \rho uv + \tau_{xy} \\ \rho uH + u\sigma_x + v\tau_{xy} - k \frac{\partial T}{\partial x} \end{bmatrix}$$

$$\mathbf{G} = \begin{bmatrix} \rho v \\ \rho uv + \tau_{xy} \\ \rho v^2 + p + \sigma_y \\ \rho vH + u\tau_{xy} + v\sigma_y - k \frac{\partial T}{\partial y} \end{bmatrix} \quad \mathbf{n} = \begin{bmatrix} n_x \\ n_y \end{bmatrix} \quad (21)$$

An in-house multi-grid N-S solver is employed to analyze the flow field around airfoil.

In this research, the high-fidelity flow model (HFFM) is a N-S equations' solution on fine grids with high degree of convergence accuracy, while the low-fidelity flow model (LFFM) is a N-S equations' solution on coarse grids with low degree of convergence accuracy. Here the fine/coarse grids are $256 \times 64 / 128 \times 48$

grids with C-mesh topology having a first grid spacing at the surface of 0.001/0.005 percent of the chord. The high/low degree of convergence accuracy means that flow calculation is performed until the maximum residual is reduced to $10^{-4} / 10^{-2}$.

For RAE2822 airfoil at $M = 0.73$, $Re = 6.5 \times 10^6$, $c_l = 0.803$, the pressure distributions predicted by the two flow models are shown in Fig.1 and the experimental data is obtained from [10]. Even though the low-fidelity flow model may not be accurate enough for performance analysis, it captures the main characteristics of the flow field and can be used for the purposes of optimization design. For RAE2822 airfoil at transonic speed, the CPU time per high-fidelity model analysis is roughly seven times the low-fidelity model analysis.

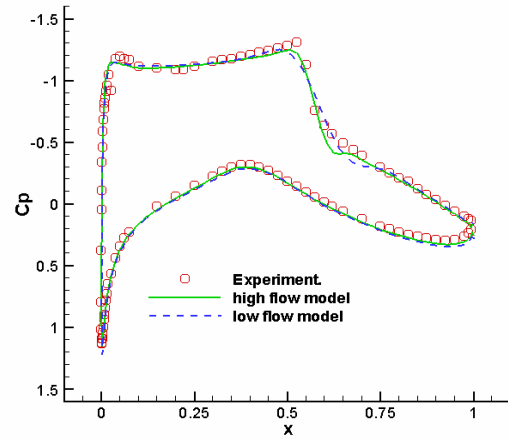


Fig. 1 RAE 2822 pressure distribution: predictions vs. experiment

4.3 Single-point design

In this study, all the designs are performed on RAE 2822 airfoil on a Hisense PC (Pentium 4 CPU 3.0GHz, RAM 1.0GB). The optimizations start from the initial point $x_0 = 0$.

The objective of the single-point design is to obtain an airfoil geometry which produces minimum transonic drag at $M = 0.73$, $Re = 6.5 \times 10^6$, $\alpha = 2.61^\circ$, meanwhile the lift and the airfoil area are not decreased. To put this design problem in the mathematical form

$$\text{Minimize } \frac{C_d}{C_{d_0}}$$

$$\text{Subject to } \frac{C_l}{C_{l_0}} - 1 \geq 0$$

$$\frac{A}{A_0} - 1 \geq 0 \quad (22)$$

where C_d and C_l are the drag and lift coefficients, respectively, A is the airfoil area, and the sub-0 indicates the value of baseline airfoil.

The results for SQP design and AMMO design are shown in Table 2 and Fig. 2.1~2.5. The strong shocks on the upper surface of baseline airfoil are removed. SQP and AMMO produce a 22.56% drag reduction respectively, while the lift and airfoil area maintain almost unchanged. AMMO produces an optimal airfoil very similar to SQP, but requires only 34.22% high-fidelity flow model evaluations and 41.36% CPU time as the SQP design.

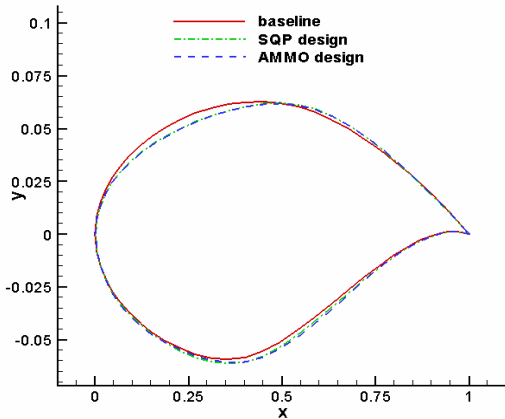


Fig. 2.1 Airfoil geometry: baseline vs. single-point designed

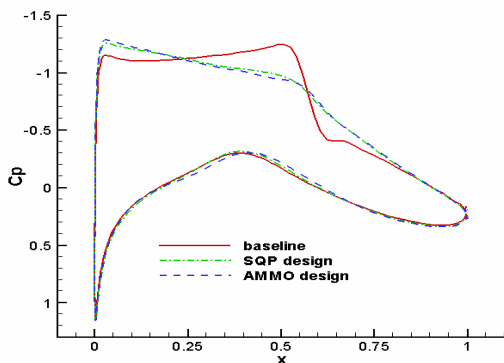


Fig. 2.2 Pressure distribution: baseline vs. single-point designed

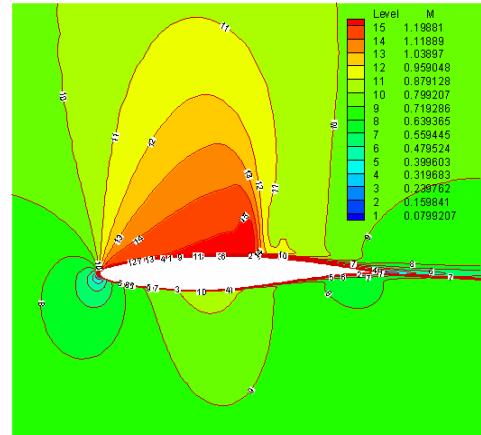


Fig. 2.3 Mach number contours: baseline airfoil

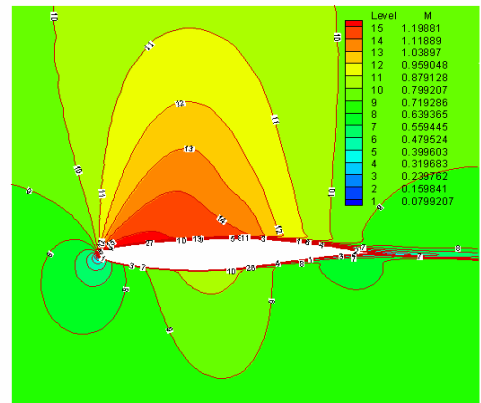


Fig. 2.4 Mach number contours: SQP designed airfoil

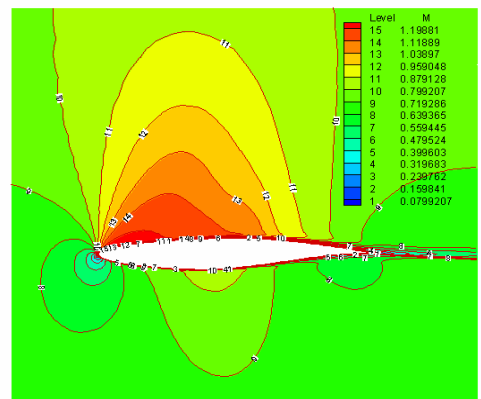


Fig. 2.5 Mach number contours: AMMO designed airfoil

Table 2 Single-point design results
for RAE 2822

Para-meter	Base-line	SQP / AMMO	Δ (%)
C_l	0.8030	0.8030 / 0.8020	0.00 / -0.12
C_d	0.0164	0.0127 / 0.0127	-22.56 / -22.56
C_m	-0.0924	-0.0904 / -0.0904	-2.16 / -2.16
A	0.0778	0.0778 / 0.0780	0.00 / 0.26
HFFM Evals		225 / 77	
LFFM Evals		0 / 315	
CPU Time		7h 18min 38sec / 3h 1min 25sec	

4.4 Multi-point airfoil design

Multi-point design improves the overall performance of the airfoil with respect to a single-point design. In this study, the objective of multi-point design is to reduce transonic drag at two design points, without decreasing the lift and airfoil area. The two design points are as following:

The primary design point, 1: $M = 0.73$, $Re = 6.5 \times 10^6$, $\alpha = 2.06^\circ$;

The secondary design point, 2: $M = 0.73$, $Re = 6.5 \times 10^6$, $\alpha = 1.56^\circ$.

To put this in the mathematical form

$$\begin{aligned} &\text{Minimize } \theta \frac{C_{d_1}}{C_{d_{10}}} + (1 - \theta) \frac{C_{d_2}}{C_{d_{20}}} \\ &\text{Subject to } \frac{C_{l_1}}{C_{l_{10}}} - 1 \geq 0 \\ &\quad \frac{C_{l_2}}{C_{l_{20}}} - 1 \geq 0 \\ &\quad \frac{A}{A_0} - 1 \geq 0 \end{aligned} \quad (23)$$

where θ is weighting parameter given according to the importance of every design point in the optimization. For this investigation, $\theta = 0.6$.

The optimization results are shown in Table 3 and Fig. 3.1~3.10. At the primary design-point, the second-order AMMO approach results in 9.60% drag reduction, 0.41% lift increasing and 1.88% pitching moment increasing, while the SQP method results in 9.60% drag reduction, 0.54% lift increasing and 2.33% pitching moment increasing. At the secondary design-point, the second-order AMMO approach results in 1.89% drag reduction, 0.00% lift increasing and 4.96% pitching moment increasing, while the SQP method results in 0.94% drag reduction, 0.00% lift increasing and 5.19% pitching moment increasing. The comparison of polar curves indicates that the two optimization procedures improve the overall characteristics of baseline airfoil evidently.

Again, the two optimization approaches obtain very similar optimal airfoils, but the high-fidelity flow model evaluations and CPU time of AMMO are only 25.86% and 28.82% as its SQP counterpart, respectively.

Table 3 Two-point design results
for RAE 2822

design point	Para-meter	Base-line	SQP / AMMO	Δ (%)
1	C_l	0.7000	0.7038 / 0.7029	0.54 / 0.41
	C_d	0.0125	0.0113 / 0.0113	-9.60 / -9.60
	C_m	-0.0903	-0.0924 / -0.0920	2.33 / 1.88
2	C_l	0.6022	0.6022 / 0.6022	0.00 / 0.00
	C_d	0.0106	0.0105 / 0.0104	-0.94 / -1.89
	C_m	-0.0887	-0.0933 / -0.0931	5.19 / 4.96
	A	0.0778	0.0778 / 0.0778	0.00 / 0.00
	HFFM Evals		642 / 166	
	LFFM Evals		0 / 424	
	CPU Time		19h 19min 57sec / 5h 34min 20sec	

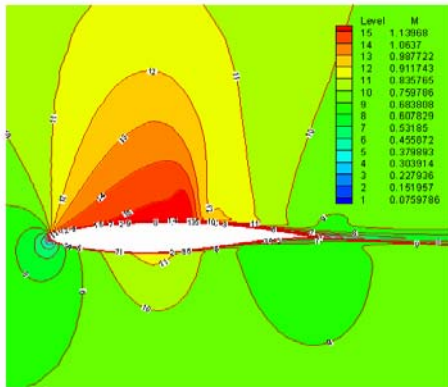


Fig. 3.1 Mach number contours at the Primary design point: baseline airfoil

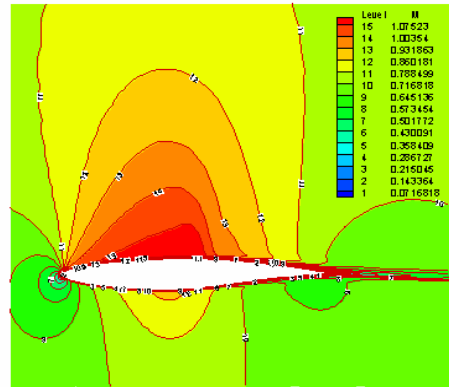


Fig. 3.4 Mach number contours at the secondary design point: baseline airfoil

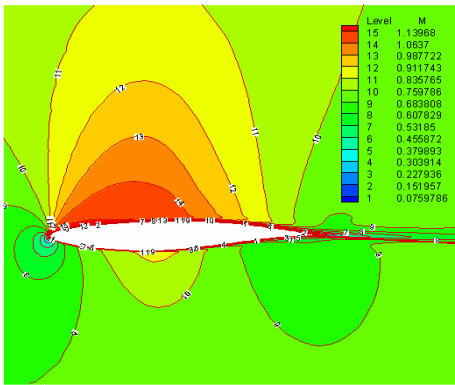


Fig. 3.2 Mach number contours at the primary design point: SQP designed airfoil

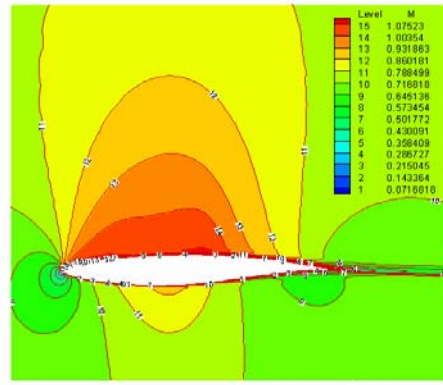


Fig. 3.5 Mach number contours at the secondary design point: SQP designed airfoil

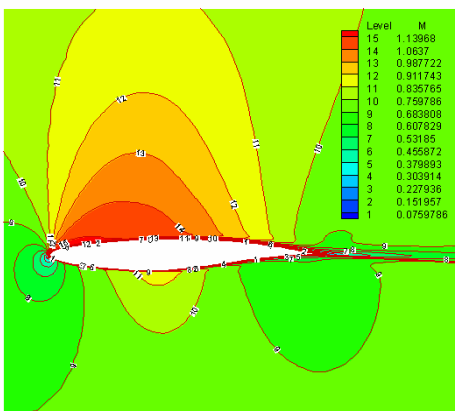


Fig. 3.3 Mach number contours at the primary design point: AMMO designed airfoil

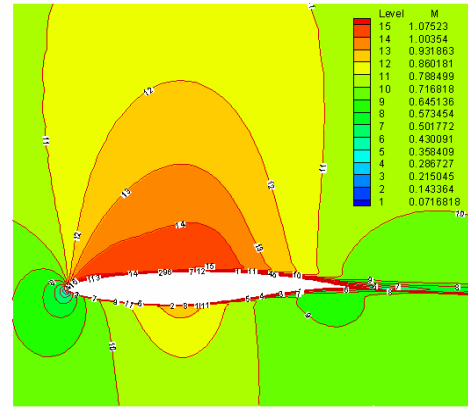


Fig. 3.6 Mach number contours at the secondary design point: AMMO designed airfoil

A VARIABLE FIDELITY OPTIMIZATION FRAMEWORK
 USING SECOND-ORDER MULTI-POINT ADDITIVE SCALING FUNCTIONS
 APPLIED TO AIRFOIL DESIGN

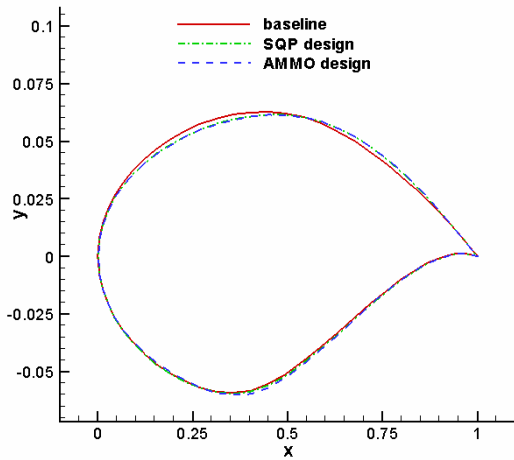


Fig. 3.7 Airfoil geometry: baseline vs. two-point designed

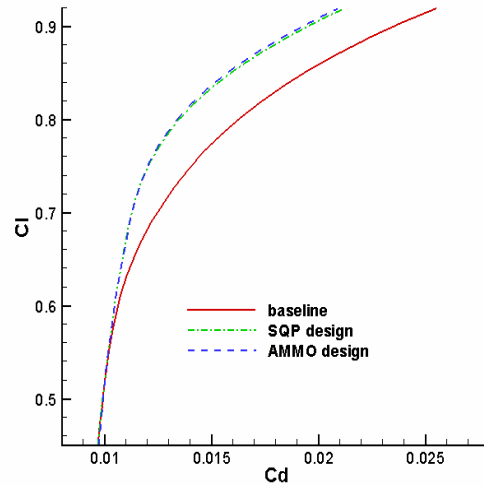


Fig. 3.10 Polar curves: baseline vs. two-point designed

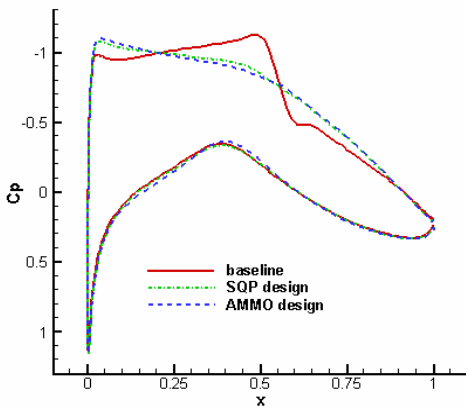


Fig. 3.8 Pressure distribution at the Primary design point: baseline vs. two-point designed

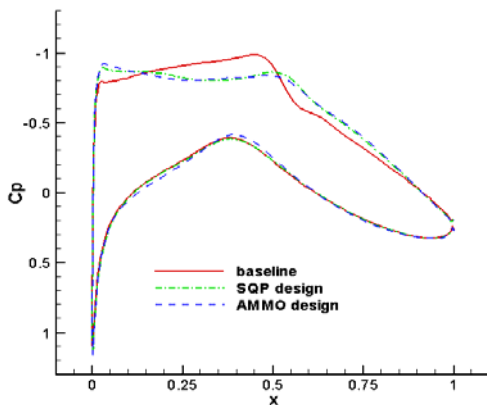


Fig. 3.9 Pressure distribution at the secondary design point: baseline vs. two-point designed

5 Conclusions

This paper describes a variable fidelity optimization framework, the second-order AMMO, which is the modification to the first-order AMMO presented by Natalia M. Alexandrov et al. The framework is based on a new second-order additive scaling function, which is a sum of quasi-Newton approximation of the high fidelity model and a term concerned to the low fidelity model and its quasi-Newton approximation. The framework can converge to the high fidelity solution at a fraction of the cost in terms of high fidelity evaluations compared to a standard SQP optimization method. Its efficiency has been preliminarily demonstrated by an analytical test problem and transonic airfoil optimization. The framework obtains very similar optimal airfoil profiles compared to SQP method, with significant performance improvement, but the CPU time are only 41.36% and 28.82% as its SQP counterpart for one point and two point airfoil design, respectively. With higher design quality, less computational expense and easier programming, the proposed variable fidelity optimization framework is suitable for performance improvement of an existing baseline airfoil to meet specified engineering requirements. As a

general procedure to design optimization, the proposed framework can also be applied in other disciplines.

References

- [1] J.O. Hager, S. Eyi, and K.D.Lee. Multi-point design of transonic airfoils using optimization. *AIAA Aircraft Design Systems Meeting*, Hilton Head, SC, AIAA 92-4225,1992.
- [2] Qian Ruizhan, Qiao Zhide et al. A practical procedure of multi-point airfoil design using SQP and Navier-Stokes equations. *Russian-Chinese aerodynamics, flight dynamics, aircraft strength conference*, Zhukovsky, Moscow Region, Russia, pp 53-58, 2003.
- [3] S.L.Lee and M.Damodaran. Airfoil design optimization using Navier-Stokes equations and simulated annealing. *22st International Congress of Aeronautical Sciences*, Harrogate, United Kingdom, ICAS2000 - 2.11.2, 2000.
- [4] J.O. Hager, S. Eyi, and K.D.Lee . Design efficiency evaluation for transonic airfoil optimization: A case for Navier-Stokes design. *AIAA 24th Fluid Dynamics Conference*, Orlando, FL, AIAA 93-3112,1993.
- [5] Natalia M. Alexandrov, Robert Michael Lewis and Clyde R. Gumbert et al. Approximation and model management in aerodynamic optimization with variable-fidelity models. *Journal of Aircraft*, Vol. 38, No. 6, pp 1093-1101, 2001.
- [6] N.M.Alexandrov, E.J.Nielsen, R.M.Lewis, and W.K.Anderson. First-order model management with variable-fidelity physics applied to multi-element airfoil optimization. *8th AIAA/USAF/NASA/ISSMO Symposium on Multidisciplinary Analysis & Optimization*, Long Beach, CA, AIAA 2000-4886,2000.
- [7] M.S.Eldred, A.A.Giunta and S.S.Collis. The second-order corrections for surrogate-based optimization with model hierarchies. *American institute of aeronautics and astronautics paper 2004-445*, 2004.
- [8] Shawn E. Gano, Victor M.Pérez, John E. Renaud and Stephen M. Batill. Multilevel variable fidelity optimization of a morphing unmanned aerial vehicle. *45th AIAA/ASME/ASCE/AHS/ASC Structures, Structural Dynamics and Materials Conference*, Palm Springs, California, AIAA 2004-1763, 2004.
- [9] Y.Yuan and W.Sun. *Optimization theory and methods*. 4st edition, Science Press, 2003 (in Chinese).
- [10] P.H.Cook, M.A.Mcdonald and C.P.Firmin. Experimental database for computer program assessment. *AGARD Advisory Report No.138*, 1979.